Wrist and Hand

4

Omid Khalilzadeh, Clarissa Canella, and Laura M. Fayad

Learning Objectives

- A basic approach to radiologic interpretation of wrist and hand imaging.
- Review of common fractures affecting the wrist and hand.
- Review of common injuries to ligamentous, tendinous, and capsular structures of the hand and wrist.

4.1 Introduction

In this chapter, we will review some of the common traumatic injuries affecting the wrist and hand. The wrist is complex, with small bones and supporting soft tissue structures, which limits the diagnostic yield for radiologic assessment [1]. A practical ABCs (alignment, bones, chondral surfaces, and soft tissues) checklist for reviewing wrist and hand exams includes assessment of alignment, bones including cortical margins, bone trabecular pattern and bone marrow signal, chondral surfaces and joints, and the soft tissues and supporting structures. Wrist alignment can be assessed by radiographs: on the frontal view (Fig. 4.1), proximal and distal carpal rows form smooth and congruent arcs, and there is mild ulnar inclination of distal radius, while on the lateral view, there is mild volar tilt of the distal radius articular surface, and the lunate bone is aligned within 10 degrees of the capitate. Evaluation of the bones is achieved through radiography, CT, and MRI, as described for different injuries below, with the bones providing boundaries to the five different compartments of the wrist (distal radioulnar joint compartment, radiocarpal compartment, midcarpal compartment, common carpometacarpal compartment, and thumb carpometacarpal compartment). When performing a wrist arthrogram (Fig. 4.2), communication of the administered contrast between any of these compartments is usually suggestive of internal derangement due to ligamentous disruption. Arthrography techniques, including MRI, are also used for assessment of the chondral surfaces.

Fig. 4.1 Three arcs drawn on the frontal radiograph of the wrist demonstrate normal alignment of the proximal and distal carpal rows

The original version of the chapter has been revised. A correction to this chapter can be found at https://doi.org/10.1007/978-3-030-71281-5_22

O. Khalilzadeh · L. M. Fayad (✉)
The Russell H. Morgan Department of Radiology and Radiological Science, The Johns Hopkins School of Medicine, Baltimore, MD, USA
e-mail: omidk@jhmi.edu; lfayad1@jhmi.edu

C. Canella
Radiology Department, Clínica de Diagnóstico por Imagem (CDPI)/DASA, Rio de Janeiro, RJ, Brazil

J. Hodler et al. (eds.), *Musculoskeletal Diseases 2021–2024*, IDKD Springer Series,
https://doi.org/10.1007/978-3-030-71281-5_4

Fig. 4.2 Wrist arthrogram images demonstrate injection of radiopaque contrast material within the midcarpal (left), radiocarpal (center), and distal radioulnar (left) compartments of wrist

In the following sections, common traumatic injuries affecting the wrist and hand are reviewed.

4.2 Metacarpal and Phalangeal Fractures

Distal phalanx fractures are the most common fractures of the hand and are frequently seen in sports injuries, such as with the mallet finger and the jersey finger. Middle phalanx fractures are the least common fractures. Proximal phalanx fractures are the most common pediatric hand fractures and can be epiphyseal or shaft fractures.

Metacarpal fractures are common, with metacarpal shaft and neck fractures typically occurring as a result of axial loading, direct trauma, or torsional force. Specific names are given to fractures of the base of the thumb metacarpal (epibasal fractures of the thumb, Bennett fracture dislocation of the thumb, and Rolando fracture of the thumb) and little finger metacarpal (reverse Bennett fracture dislocation fracture and boxer fracture) [2].

Mallet finger: The mallet finger results from disruption of the terminal tendon contribution to the extensor mechanism of the finger at its attachment to the dorsal aspect of proximal phalangeal base, with or without bony avulsion [3]. These are the most common tendon injuries in sports, resulting from a combination of pulling force at the terminal tendon combined with extension of distal interphalangeal joint. Radiographs may show a tiny avulsed bone fragment, and ultrasound may show loss of real-time movement of the tendon.

Seymour fracture: This is a pediatric subtype of the mallet finger with distal phalanx physeal fracture and associated nail bed injury, most commonly occurring with ungual subluxation.

Jersey finger: The Jersey finger (Fig. 4.3) results from disruption of the flexor digitorum profundus at the volar base of distal phalanx, with or without a bony avulsion [4]. The avulsed tendon or bone fragment may be retracted proximally, most commonly up to the edge of the A2 pulley along the proximal phalanx. It usually occurs in sports secondary to forceful hyperextension of a flexed finger during activity.

Fig. 4.3 Jersey finger with avulsion fracture of the volar base of distal phalanx and proximal retraction to the edge of A4 pulley

Bennett fracture dislocation: This is a two-piece fracture of the base of the thumb metacarpal with intra-articular extension and dorsolateral displacement. A small ulnar fragment of the thumb metacarpal, attached to the anterior oblique ligament of the thumb carpometacarpal bone, remains in place articulating with the trapezium.

Fig. 4.4 Fracture of fifth metacarpal neck compatible with boxer fracture

Rolando fracture dislocation: This can be categorized as a comminuted form of the Bennett fracture. This is a three-part, intra-articular fracture dislocation of the base of the thumb. The fracture line is typically a Y or T shape, and a volar fragment remains in articulation.

Epibasal fractures of the thumb: This is a two-piece fracture of the base of the thumb. These fractures are usually stable and often do not require surgery, in contrast to the above Bennett and Rolando fractures.

Boxer fracture: This is a fracture of fifth metacarpal neck (Fig. 4.4), commonly secondary to direct longitudinal trauma, such as boxing injury.

Reverse Bennett fracture dislocation: This is a fracture dislocation of the base of the fifth metacarpal.

Key Point

- Phalanx and metacarpal fractures are common and are usually seen with sports injuries. Intra-articular extension and injury to joint capsular ligaments, tendons, or physeal plates are commonly seen with these fractures.

4.3 Carpal Fractures

Carpal bone fractures can involve one or a combination of carpal bones, usually seen as part of carpal fracture dislocations [5]. Individual fractures include the following fractures:

Scaphoid fracture: This is the most common carpal bone fracture (Fig. 4.5) and may be occult on radiographs. Fractures are usually secondary to a fall on an outstretched hand and may involve the waist of the scaphoid (70–80%), distal pole of scaphoid tubercle (20%), or proximal pole (10%). Arterial supply to the scaphoid is from distal to proximal pole. Therefore, the more proximal the site of fracture, the higher likelihood of malunion/non-union, avascular necrosis of the proximal fragment, and long-term complications such as SNAC wrist (scaphoid nonunion advanced collapse) and SLAC wrist (scapholunate advanced collapse) (Fig. 4.6).

Triquetral fracture: This is the second most common carpal fracture after the scaphoid. The most common fracture of the triquetral bone is a dorsal avulsion fracture at the attachment of radiocarpal ligament, secondary to fall on an outstretched hand, best seen on lateral view. Triquetral body or volar avulsion fractures are less commonly seen fractures.

Lunate fracture: This fracture is usually secondary to axial loading and could involve the volar pole, dorsal pole, or body. Non-displaced transverse fractures through the body of the lunate have been known as a predisposing factor to avascular necrosis of lunate, particularly in patients with negative ulnar variance who receive more axial loading on the lunate through contact with the distal radius.

Hook of hamate fracture: This type of fracture (Fig. 4.7) may occur due to a direct trauma during sports or a fall and may result in Guyon's canal syndrome. A hook of hamate fracture is best identified on axial cross-sectional imaging, with MRI or CT, through the wrist.

Tubercle of trapezium fracture: The most common site of fracture is the tubercle of trapezium (Fig. 4.8) at its volar surface.

Trapezoid, pisiform, and capitate fractures: These fractures are less commonly seen in isolation.

Combination fractures: These fractures involve more than one carpal bone and may be associated with a dislocation [6].

4.3.1 Perilunate Injuries

Due to dynamic alignment and ligament support of the wrist, transmission of force through the carpus (usually via axial loading, dorsiflexion, ulnar deviation, and supination) can

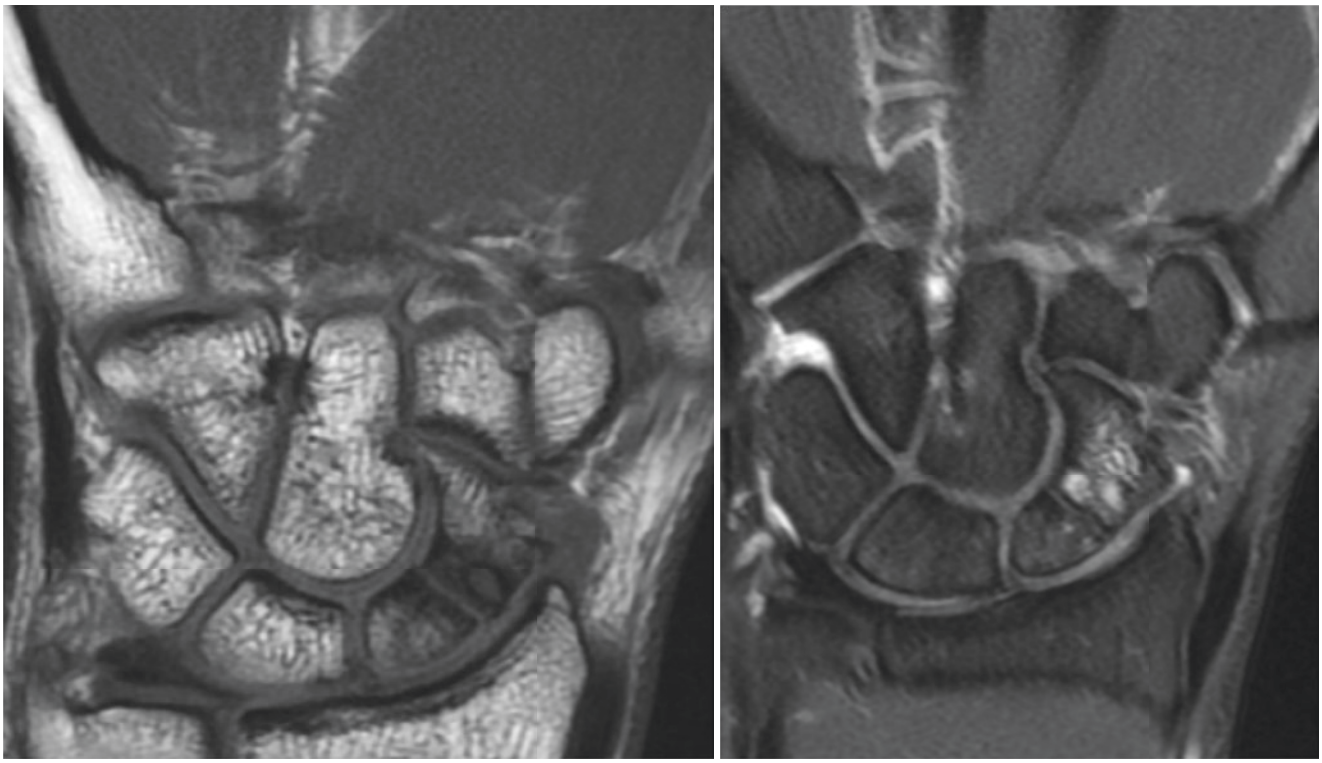

Fig. 4.5 Scaphoid fractures could be occult on radiographs. Coronal MR images through the wrist demonstrate a chronic appearing minimally displaced fracture of scaphoid wrist

Fig. 4.6 Severe case of scapholunate advanced collapse (SLAC), commonly known as SLAC wrist. Coronal fluid-sensitive MR image through the wrist demonstrates widening of the scapholunate interval compatible with scapholunate ligament tear, with associated proximal migration of capitate and advanced secondary degenerative changes of radioscaphoid articulation

cause a sequence of injuries through a perilunate *zone of vulnerability* in the wrist, as described by Mayfield et al. [7]. Two different sets of injuries can occur in the wrist "zone of vulnerability" (Fig. 4.9):

1. **Lesser arc injuries:** These are usually related to rapid transmission of force and are purely ligamentous.
2. **Greater arc injuries:** These are usually related to slower transmission of force and include fractures as well as ligament injuries.

Perilunate injuries can result in volar dislocation of the capitate with respect to the lunate which could progress from stage I **scapholunate dissociation** to stage II, dorsal **perilunate dislocation**; stage III, **midcarpal dislocation**; and finally stage IV, volar **lunate dislocation** (Fig. 4.10).

Lesser arc perilunate injuries occur in a sequence which is called progressive perilunate failure. These injuries start at the scapholunate joint, then proceed to the lunocapitate and lunotriquetral joints, and finally culminate in complete dislocation of the lunate.

Perilunate injury with associated fracture of one or more bones around the lunate (scaphoid, trapezium, capitate, hamate, or triquetrum) is called a greater arc injury. Greater arc injuries could have trans-radial, trans-scaphoid, trans-capitate, trans-triquetrum, or trans-ulnar styloid components in association.

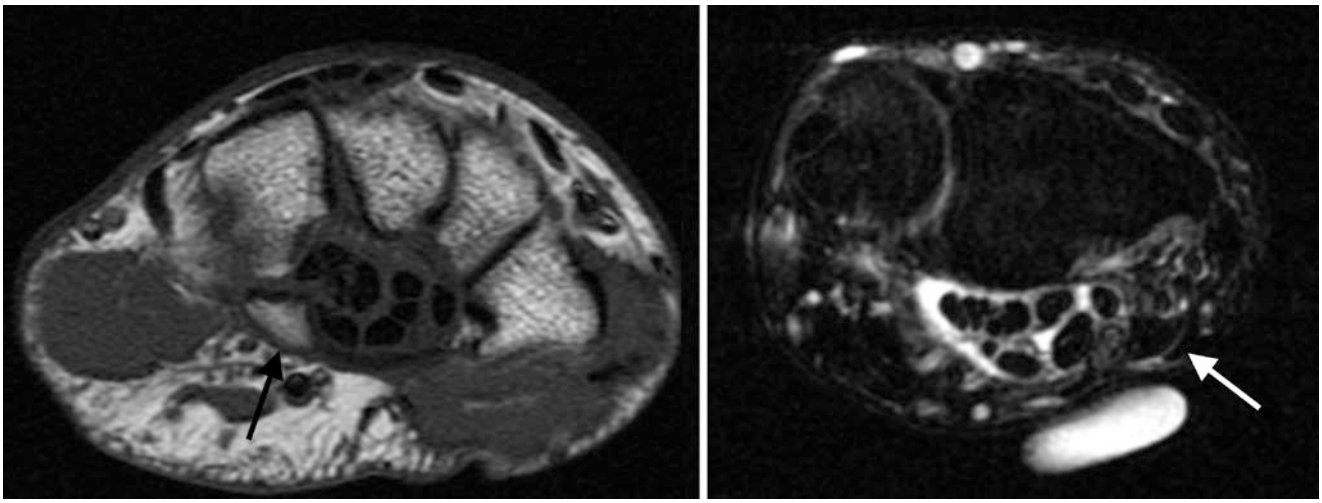

Fig. 4.7 Axial MR images demonstrate a mildly displaced fracture of hook of hamate. Lack of edema like signal and corticated margins are suggestive of a chronic fracture

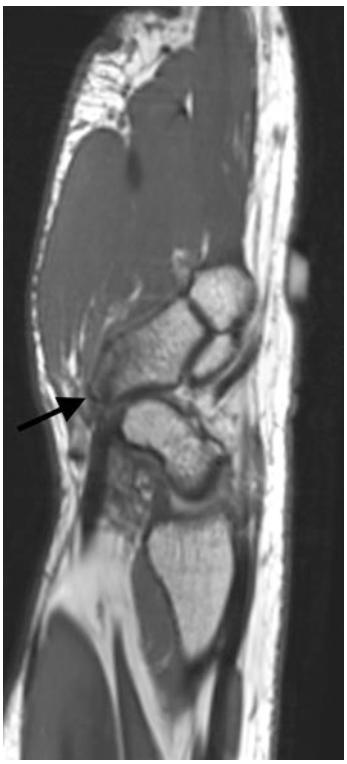

Fig. 4.8 Sagittal T1-weighted MR image demonstrates a non-displaced fracture of tubercle of trapezium

Fig. 4.9 Wrist is vulnerable to injuries through a perilunate "zone of vulnerability" (red zone). Two different sets of injuries can occur along this zone, as depicted by dash lines: lesser arc injuries and greater arc injuries

Key Point

- Carpal fractures may involve one individual bone or more than one carpal bone, as part of the commonly seen perilunate injuries through the zone of vulnerability. Perilunate injuries may be associated with dislocation.

4.3.2 Carpal Instability

By terminology, instability is a dynamic process and requires dynamic assessment of carpal bones in motion, often evaluated by dynamic fluoroscopy. What is commonly evaluated on static radiologic images is malalignment which is a manifestation of dynamic instability. Therefore, radiology

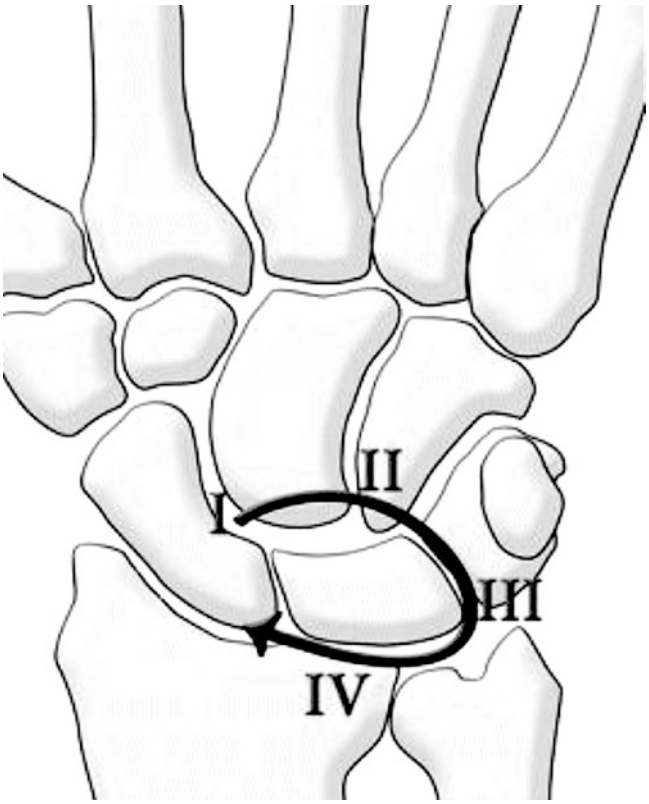

Fig. 4.10 Four stages of progressive perilunate injury: stage I, "scapholunate dissociation"; stage II, dorsal "perilunate dislocation"; stage III, "midcarpal dislocation"; and finally stage IV, volar "lunate dislocation"

reports describe the findings as "malalignment which is seen with a certain clinical pattern of carpal instability."

Different classifications have been suggested for carpal instability [8], as below:

The Mayfield classification of carpal instability: This classification system is also known as perilunate instability, which is focused on perilunate patterns of carpal instability [7]. Other forms of carpal instability such as adaptive instability secondary to an extracarpal factor are not included in this classification.

Under this classification, instability is divided into four stages:

- Stage I: scapholunate dissociation.
- Stage II: perilunate dislocation, with the lunate remaining normally aligned with the distal radius and the remaining carpal bones dislocated dorsally.
- Stage III: midcarpal dislocation, where neither the capitate nor the lunate is aligned with the distal radius.
- Stage IV: lunate dislocation, which is usually volar (Fig. 4.11).

The Mayo classification of carpal instability: This scheme offers a more comprehensive classification, divided into four categories [9].

- Dissociative (CID): dissociation of bones of the same carpal row, in the mediolateral direction.
  - Scapholunate dissociation, which is the most common cause of dorsal intercalated segment instability (DISI) (Fig. 4.12).
  - Lunotriquetral dissociation, which is the most common cause of volar intercalated segment instability (VISI).
  - Distal dissociative carpal instability.
- Non-dissociative (CIND): structural derangement between the proximal carpal row and the radius or the distal carpal row with a normal relationship of the carpal bones within that row. Typically, with CIND, there is dissociation in a direction other than mediolateral.
  - Radiocarpal instability, including ulnar or radial translocation, or radiocarpal dislocation.
  - Midcarpal instability, including volar or dorsal midcarpal instability.
- Complex (CIC): CID and CIND combined, including dorsal or volar perilunate dislocation or fracture dislocation, i.e., greater or lesser arc injury.
  - Axial dislocations (high energy trauma, e.g., peritrapezium or perihamate).
- Adaptive (CIA): Dissociation occurs secondary to extrinsic causes including proximal or distal causes such as distal radius fracture malunion or madelung deformity.

The articulations between the lunate and the surrounding four bones play the most important role in carpal stability. When evaluating carpal instability, attention should be focused on lunate articulations, including radiolunate, lunocapitate, lunotriquetral, and scapholunate. Each articulation should be assessed for signs of displacement or malrotation. Measurement of carpal angles between the lunate and other bones including radiolunate, scapholunate, and lunocapitate could be used as a hint to carpal malalignment. For example, malalignment at the radiolunate is seen with radiocarpal instability. Malalignment at the lunocapitate articulation is seen with midcarpal instability.

Please note that perilunate instability is not interchangeable with midcarpal instability. The former may include dissociation within the proximal carpal row. However, the latter is a non-dissociative instability. The key feature in midcarpal instability is lunocapitate malalignment which may or may not be seen in perilunate instability.

4.4 Tendon Injuries

Flexor tendon and extensor mechanism anatomy of the hand is demonstrated in Fig. 4.13. Common conditions involving the tendons of the hand and wrist include a trigger finger, tenosynovitis of the first through sixth dorsal extensor

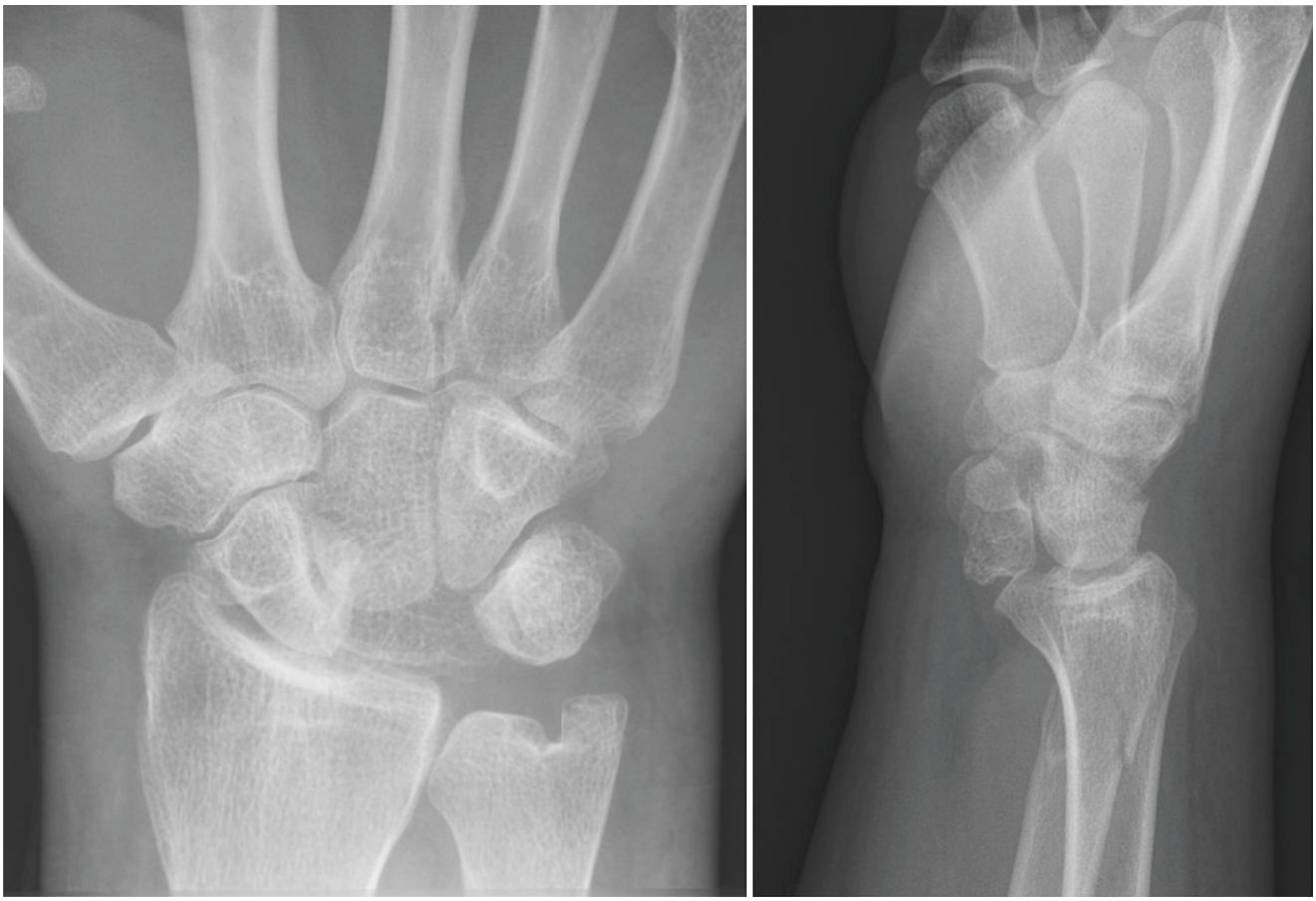

Fig. 4.11 Frontal and lateral radiographs demonstrate volar dislocation of lunate. Notice disruption of carpal arcs on the frontal view. Additional fracture of distal radius is visible on the lateral radiograph

compartments, and flexor carpi radialis tendonitis. Tendinosis is chronic degeneration of a tendon due to mechanical stress and repetitive trauma. Laceration followed by avulsion injuries is the main cause of traumatic injuries to tendons. Tenosynovitis is fluid expansion and synovitis of a tendon sheath, which could be due to degenerative, infectious, or inflammatory etiologies [10, 11].

4.4.1 Extensor Carpi Ulnaris Tendon (ECU) Injury

It is important to differentiate between ECU subluxation and normal dynamic variations in positioning. ECU position within the ulnar groove is dependent on wrist position. ECU is in ulnar position on pronation and in radial position in supination. ECU dislocation is secondary to ECU subsheath injury, including tears of the radial or ulnar roots of the ECU subsheath. ECU tendinosis and tear (Fig. 4.14) are the most common tendon pathologies of the hand and wrist.

Stenosis tenosynovitis: Stenosing tenosynovitis develops secondary to chronic repetitive microtrauma from frequent movements of the tendons, through osseofibrous tunnels, such as with the overlying retinaculum or pulley [10].

De Quervain's tenosynovitis: This is a common form of stenosing tenosynovitis involving the first extensor tendon compartment (abductor pollicis longus (APL) and extensor pollicis brevis (EPB) tendons) of the wrist, typically at the radial styloid (Fig. 4.15). The most common etiology is thickening of the overlying extensor retinaculum at the radial styloid.

Trigger finger: This is a type of stenosing tenosynovitis involving the flexor digitorum superficialis at the level of the A1 pulley. Ultrasound can show real-time impingement of the tendon while gliding through its tunnel, and there is thickening of the overlying flexor pulley measuring >1–1.5 mm.

Intersection syndrome: At the crossing point of the first dorsal compartment (APL and EPB) and second dorsal compartment (ECRL, ECRB), tenosynovitis occurs and is known as proximal intersection syndrome. Tenosynovitis at the third compartment (extensor pollicis longus, EPL) and second dorsal compartment (ECRL, ECRB) crossing point is known as distal intersection syndrome.

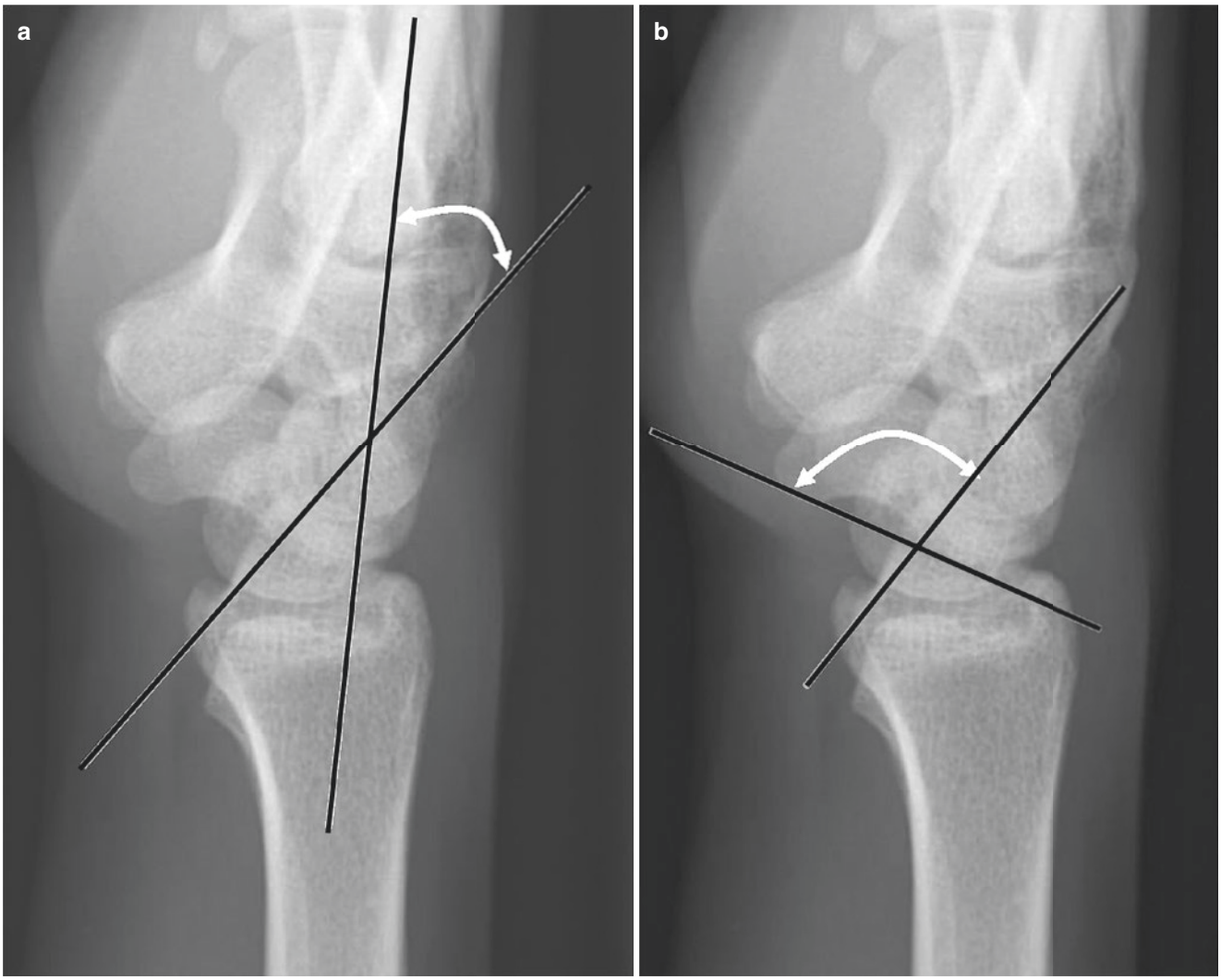

Fig. 4.12 Lateral radiographs demonstrate volar tilt of lunate with widening of capitolunate angle >30° and scapholunate angle >60° (**a** and **b**, respectively) compatible with malalignment seen with dorsal intercalated segment instability (DISI)

Pulley injuries: Pulleys are fibrous structures which wrap around the flexor tendon sheaths of the digits to form a supporting fibro-osseous tunnel (Fig. 4.16). Five such annular pulleys (A1–A5), together with three cruciate pulleys (C1–C3), form a fibro-osseous tunnel. Cruciate pulleys are difficult to find on imaging due to their thin size, and injuries are less commonly discussed. However, the A2 pulley is the most load bearing and most commonly injured pulley and can be identified by imaging, particularly axial non-fat-suppressed T1- or intermediate-weighted imaging. A1, A3, and A5 pulleys attach to volar plates at the level of metacarpophalangeal (MCP), proximal interphalangeal (PIP), and distal interphalangeal (DIP) joints and are less commonly torn. A2 and A4 pulleys attach to the periosteum at the proximal and middle phalanx. Pulley sprain or rupture can be associated with bowstringing of the flexor digitorum tendons, and increased bone-tendon distance is best detected on sagittal images.

Boutonniere deformity: "Boutonnière" is French for buttonhole. Increasing PIP joint flexion causes further extensor retinaculum damage resulting in "buttonholing" of the proximal phalanx between the lateral bands of the extensor tendon. Secondary DIP joint extension then occurs. Findings result from rupture of the central slip of the extensor mechanism from its attachment at the dorsal base of the middle phalanx or failure of the triangular ligament.

Key Point

- Common conditions involving the tendons of the hand and wrist include trigger finger, tenosynovitis of the first through sixth dorsal extensor compartments, and flexor carpi radialis tendonitis.

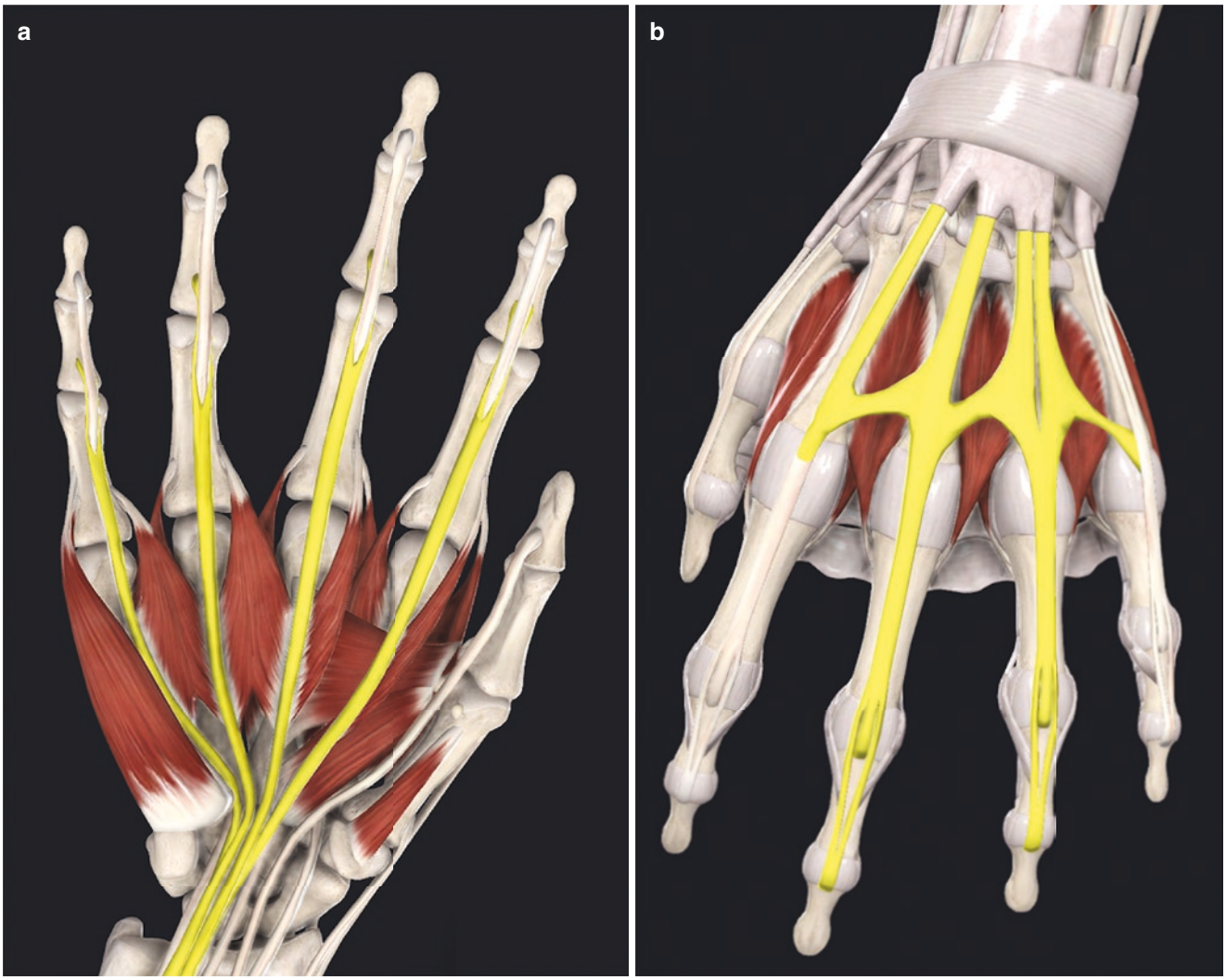

Fig. 4.13 Flexor (**a**) and extensor tendon (**b**) anatomy of the hand. Flexor digitorum superficialis (FDS) divides into two medial and lateral slips (yellow) and attaches to the base of the middle phalanx. Flexor digitorum profundus (FDP) attaches to the base of the distal phalanx. The extensor hood forms a central slip, which attaches to the base of the middle phalanx, and two lateral bands join together to form a terminal tendon, which attaches to the base of distal phalanx

4.5 Ligaments and Capsular Injuries

Volar and dorsal plate injuries: The most commonly injured site is the volar plate of the PIP joints. A hyperextension injury may result in a ligament tear or an intra-articular avulsion fracture.

Collateral ligament injuries: Collateral ligaments have two components: main (proper) and accessory. Forced ulnar or radial deviation at any of the interphalangeal joints can cause collateral ligament tears, best detected by MRI.

Sagittal band injuries: Sagittal band rupture can be evaluated on axial slice T1-weighted or intermediate-weighted non-fat-suppressed images. Rupture of the sagittal band leads to medial or lateral dislocation of the extensor tendon at the level of the MCP joint.

Gamekeeper's thumb and Stener lesion: This is an avulsion or rupture of the ulnar collateral ligament of the thumb MCP joint. MRI plays a key role in differentiating a simple collateral ligament injury from a Stener lesion, which requires surgical treatment. In simple injury, the adductor pollicis aponeurosis remains superficial to the torn collateral ligament. In a Stener lesion (Fig. 4.17), the adductor pollicis aponeurosis is interposed between the torn end of the ulnar collateral ligament and the base of the proximal phalanx, interfering with the healing process and warranting a surgical intervention [12].

Injury to extrinsic and intrinsic carpal ligaments: Carpal ligaments (Fig. 4.18) play a vital role in stability of the wrist [13]. Carpal ligaments are classified as intrinsic (when only attached to carpal bones) and extrinsic (when

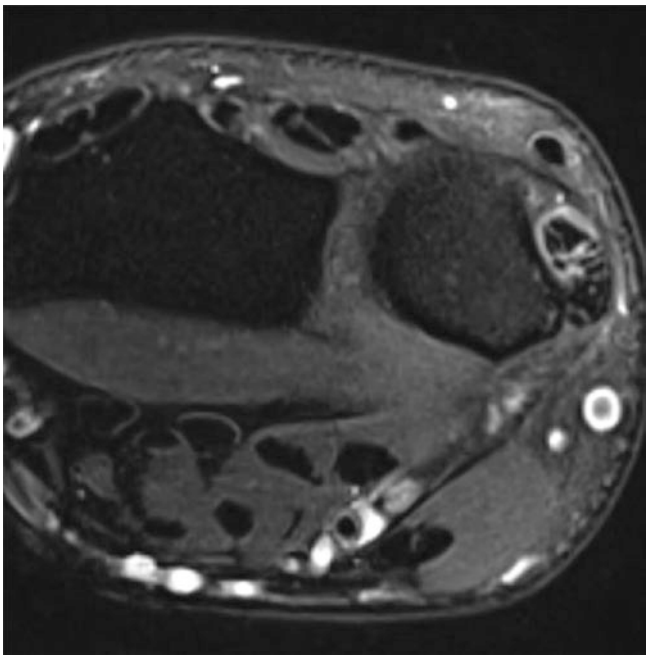

Fig. 4.14 Fluid-sensitive MRI images through the wrist demonstrate tendinosis and mild tenosynovitis of extensor carpi ulnaris with a superimposed partial thickness longitudinal tear

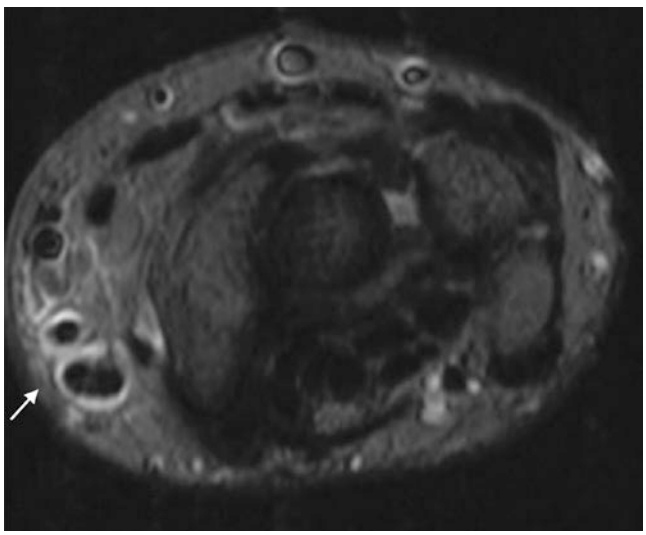

Fig. 4.15 Axial fluid-sensitive MR images demonstrate tenosynovitis of the first extensor compartment at the level of radial styloid process compatible with De Quervain's tenosynovitis

attached to structures outside the carpus). Of the proximal interosseous ligaments, the scapholunate and lunotriquetral ligaments are the most important intrinsic carpal ligaments and are best assessed by MRI.

Scapholunate ligament injury: The scapholunate ligament is a U-shaped ligamentous complex with three components: dorsal, volar, and interosseous components. The dorsal component is the thickest component and is more commonly injured. Failure of this ligament results in rotary subluxation of the scaphoid, with volar rotation of the scaphoid and dorsal rotation of the lunate (DISI instability as discussed above).

Fig. 4.16 Pulleys are fibrous structures which wrap around the flexor tendon sheaths of the digits to form a supporting fibro-osseous tunnel. Five such annular pulleys (A1–A5), together with three cruciate pulleys (C1–C3), form a fibro-osseous tunnel along each finger

Lunotriquetral ligament injury: Lunotriquetral ligament is a U-shaped ligamentous complex with three components: dorsal, volar, and interosseous components. Volarly it blends with the ulnocarpal ligaments as part of the triangular fibrocartilage complex (TFCC). The volar component is the thickest component and is more commonly injured. Failure of this ligament results in volar rotation of the lunate (VISI instability as discussed above).

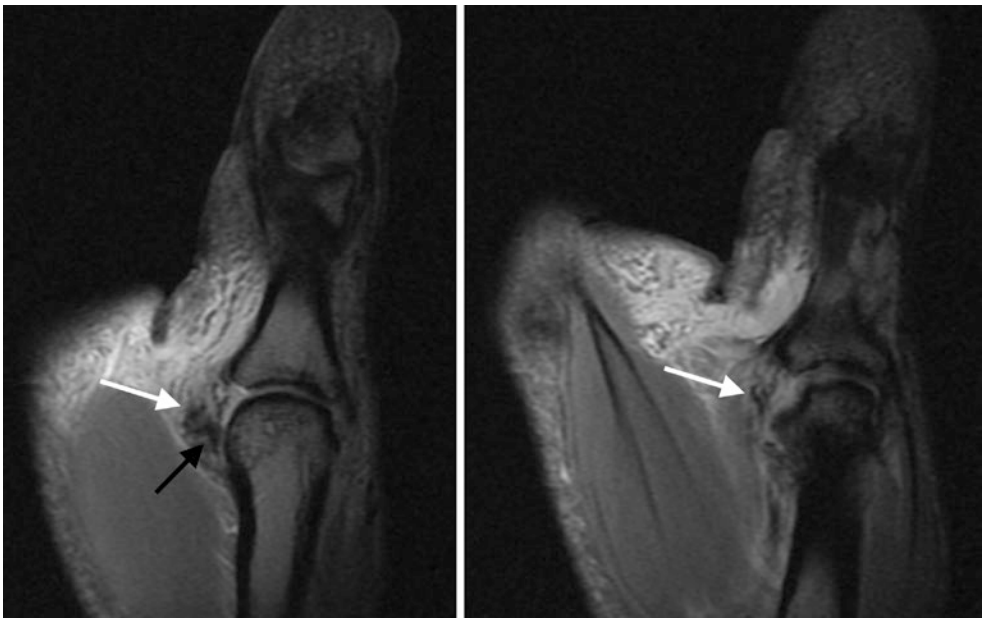

Fig. 4.17 Stener lesion. Coronal fluid-sensitive MRI images through the thumb demonstrate full-thickness tear of ulnar collateral ligament (white arrow) with the adductor pollicis aponeurosis interposed between the torn end of the ulnar collateral ligament and the base of the proximal phalanx (black arrow)

4.6 Miscellaneous Topics

Ulnar variance: Ulnar variance is measured in neutral wrist position on radiographs and refers to a relative distal projection of the distal ulnar articular surface with respect to the radius [14]. In a neutral variance wrist, approximately 80% of axial loading passes through the radius, and 20% passes through the ulna. A positive ulnar variance is associated with more axial loading through the ulna which results in ulnocarpal impaction and TFC wear and tear. A negative ulnar variance results in more axial loading through the radius to the lunate and scaphoid and may be associated with avascular necrosis of lunate.

Triangular fibrocartilage complex (TFCC) tear: TFCC is a complex structure (Fig. 4.19) with several components supporting a central triangular-shaped fibrocartilage, known as the TFC, or disk proper portion of TFCC. The TFC is attached dorsally and volarly to radioulnar ligaments supporting it on the sides like a hammock between the sigmoid notch and the ulnar styloid. The dorsal and volar radioulnar ligaments extend from the dorsal and volar edges of the ulnar styloid process to the dorsal and volar edges of the sigmoid notch of the distal radius, respectively. Dorsally, the dorsal radioulnar ligament blends with the ulnomeniscal homologue which extends ulnarly to form a meniscus-shaped styloid component. The styloid component extends distally and forms a collateral component which joins with the ulnar collateral ligament and ECU subsheath and attaches to triquetrum distally [15]. Dorsally, the dorsal radioulnar ligament, ulnomeniscal homologue, and ulnar collateral ligaments blend with the ECU subsheath. Volarly, the radiocarpal ligament blends with the ulnocarpal ligaments. The TFC is attached to the ulna via two laminar attachment points which are in continuity with radioulnar ligaments: the proximal lamina, which connects to the fovea, and distal lamina which connects to the ulnar styloid. The fibers interposed between the proximal and distal lamina are referred to as the ligamentum subcruentum. Injuries to the TFCC have been described in the Palmer classification as traumatic or degenerative [16].

The blood supply for the TFC is from periphery to its central aspect. Therefore, its central aspect is most prone to degeneration and degenerative central perforation. The peripheral portion is more vascular and may repair following injury.

An acute TFCC injury may involve the TFC and any of the complex supporting components detailed above. Common patterns of acute TFCC injury include central perforation, peripheral or ulnar sided tear, distal tear or tear of ulnocarpal ligaments, and a radial disruption at sigmoid notch. TFCC tear is usually evaluated on coronal and sagittal fluid-sensitive pulse sequences of MRI.

A common pattern of chronic TFCC tear associated with degeneration is seen with ulnar impaction syndrome, as detailed below.

Ulnar impaction syndrome: Known as ulnar abutment or ulnocarpal impaction (Fig. 4.20), this syndrome results from impaction of the ulna on the proximal articular aspect of the lunate [17]. Etiologies include a positive ulnar variance associated with excessive axial loading. The spectrum of findings includes TFC complex wear and tear, lunotriquetral tear, ulnolunate cartilage disease, and ultimately secondary ulnocarpal degenerative joint disease.

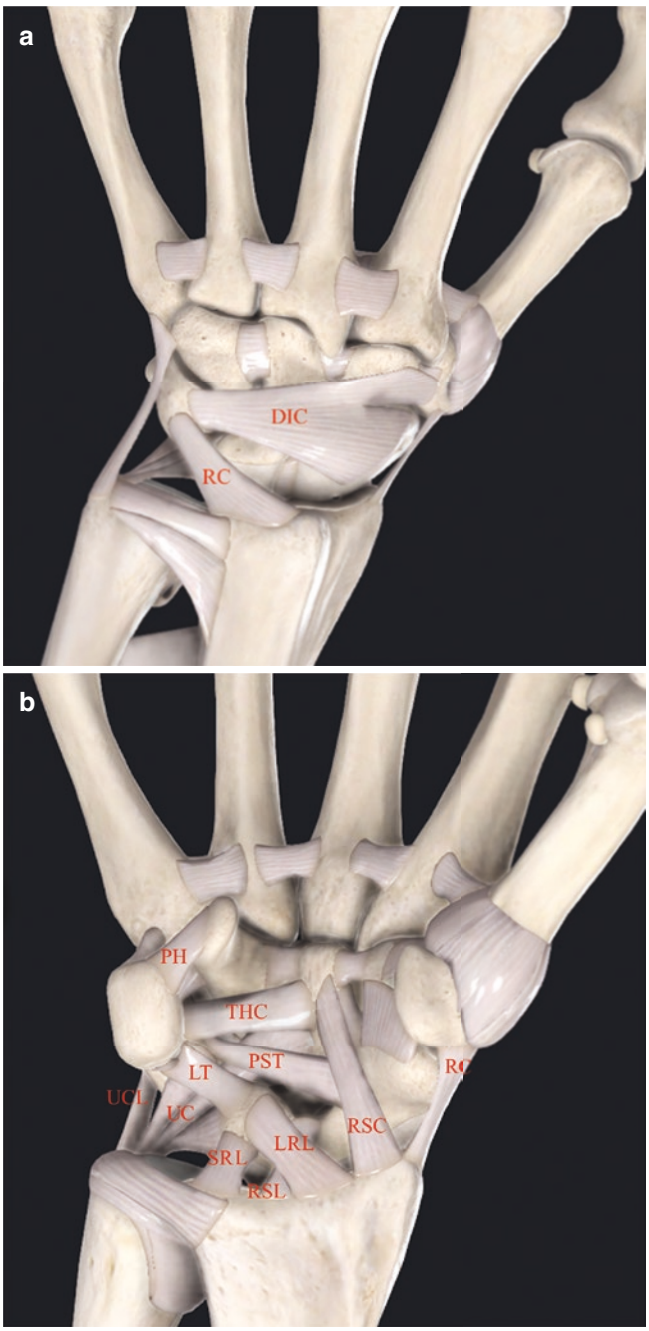

Fig. 4.18 Carpal ligaments. Major dorsal carpal ligaments (**a**) include dorsal intercarpal (DIC) ligament and dorsal radiocarpal ligament (DRC). Major volar carpal ligaments (**b**) include radioscaphocapitate (RSC), long radiolunate ligament (LRL) or radiolunotriquetral ligament, radioscapholunate (RSL), short radiolunate (SRL), and ulnocarpal (UC) ligaments. Triquetrohamocapitate (THC), radial collateral ligament (RC), ulnar collateral ligament (UCL), lunotriquetral (LT), palmar scaphotriquetral ligament (PST), and pisohamate (PH) are also demonstrated

Ulnar impingement syndrome: This syndrome results from a shortened distal ulna impinging on the distal radius proximal to the sigmoid notch, causing secondary degenerative changes including surface remodeling, marginal osteophyte formation, and bone marrow edema [18]. Etiologies of this syndrome include negative ulnar variance, a madelung deformity, or surgical resection of the distal ulna.

Hamatolunate impaction: Secondary degenerative changes with chondral loss and subchondral bone marrow edema at the hamatolunate articulation occur in patients with type II lunate [19]. A type II lunate is the existence of a medial facet on the distal lunate for articulation with the hamate.

Avascular necrosis: Kienböck disease (Fig. 4.21) is the eponymous name given to avascular necrosis of the lunate. Post-traumatic avascular necrosis of the scaphoid is discussed above as well.

Key Point

- Ulnar variance should be assessed with wrist in neutral position. Positive and negative ulnar variance is associated with variation in the axial loading balance of the distal radius and ulna and may result in different conditions, including ulnar impingement, ulnar impaction, and TFCC wear.

4.6.1 Systemic Diseases

Many systemic diseases including rheumatologic conditions, inflammatory arthropathy, crystal arthropathy, and metabolic diseases demonstrate manifestations in the hands and wrists. Discussion of these entities is beyond the scope of this chapter. These disorders are associated with synovitis (Fig. 4.22) in the various compartments of the wrist as well as tenosynovitis (well depicted by MRI) and periarticular erosions, which lead to ligamentous injuries and various patterns of deformity, such as a SLAC wrist.

4.7 Concluding Remarks

This chapter reviews traumatic injuries of the hand and wrist, highlighting that chronic rheumatologic conditions can be associated with similar manifestations. Knowledge of anatomy is key to the diagnosis in wrist and hand imaging, and usually, a combination of different imaging modalities may be needed to effectively diagnose osseous and soft tissue injuries. Radiographs can show the overall alignment, margins at the matrix of osseous lesions, presence or absence of mineralization, and differentiation of ossific from calcific opacities, including avulsion fractures. Computed tomography can better assess radiographically occult fractures and

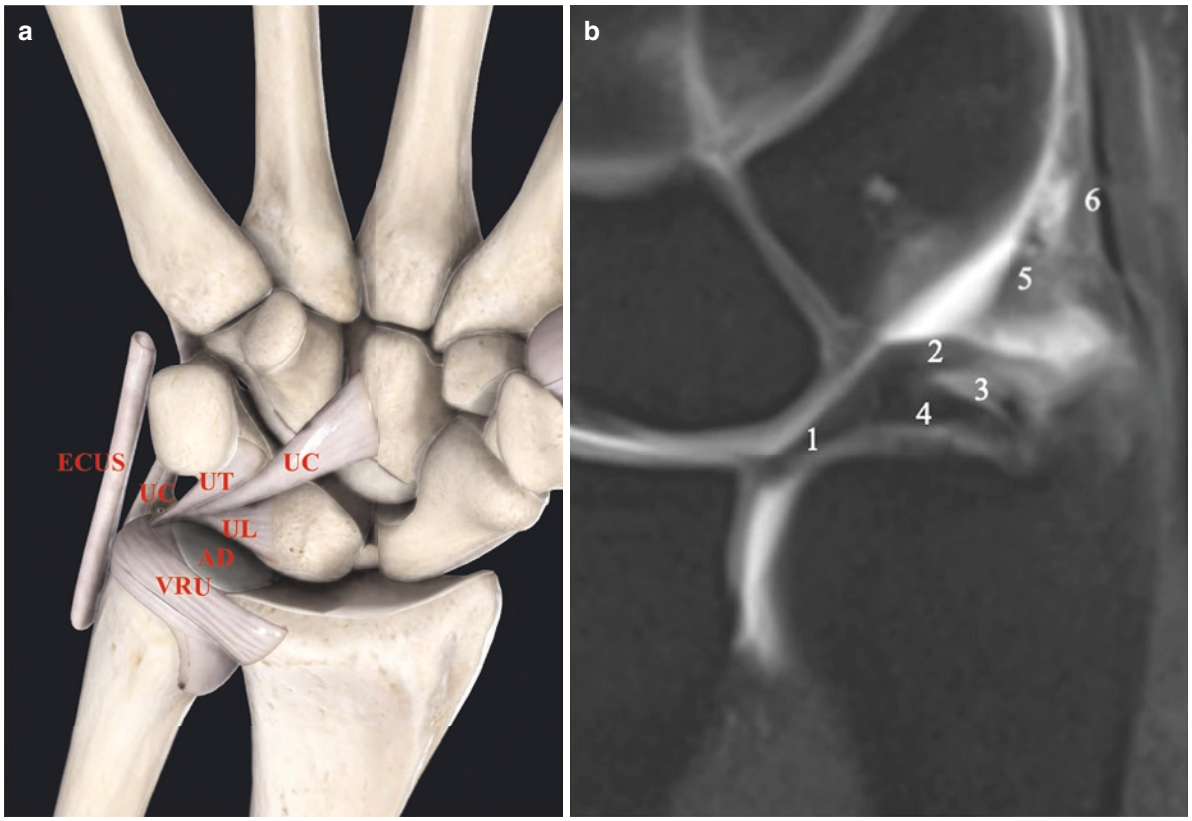

Fig. 4.19 Schematic (**a**) and coronal MR (**b**) images demonstrate some of the major components of the triangular fibrocartilage complex (TFCC), including articular disk (AD), volar radioulnar ligament (VRU), and ulnocarpal ligaments (UT, ulnotriquetral; UL, ulnolunate; and UC, ulnocapitate). Extensor carpi ulnaris subsheath (ECUS) and ulnar collateral ligament are also demonstrated. The numbers correspond to the following: (1) articular disc portion of TFCC; (2) distal lamina; (3) ligamentum subcruentum; (4) proximal lamina; (5) ulnomeniscal homologue; and [6] ulnar collateral ligament

Fig. 4.20 Coronal fluid-sensitive MR image demonstrates positive ulnar variance with associated degenerative central perforation of triangular fibrocartilage and subchondral cystic changes/bone marrow edema of the proximal articular aspect of lunate, compatible with ulnar abutment syndrome

show more details regarding bony alignment and the status of posttraumatic healing, osseous bridging, or complications related to fixation hardware. Magnetic resonance imaging best depicts the bone marrow signal and complex anatomy of the supporting soft tissue structures. And finally, ultrasound can add value as a method for real-time functional evaluation of the tendons and ligaments.

Take Home Messages

- Knowledge of wrist and hand anatomy is key to diagnosis. Some of the essential anatomic and clinical topics include topographic tendon anatomy of the wrist and hand, intrinsic and extrinsic carpal ligaments, collateral ligaments, triangular fibrocartilage complex, extensor mechanism, flexor tendon, and pulleys.
- Many systemic diseases including rheumatologic conditions, inflammatory arthropathy, crystal arthropathy, and metabolic diseases demonstrate manifestations in the hands and wrists. Differentiating an acute injury on a background of underlying disease may sometimes be challenging.

Fig. 4.21 Coronal MR images through the wrist demonstrate bone marrow edema-like signal and low signal sclerotic change involving the lunate compatible with avascular necrosis, Kienböck disease

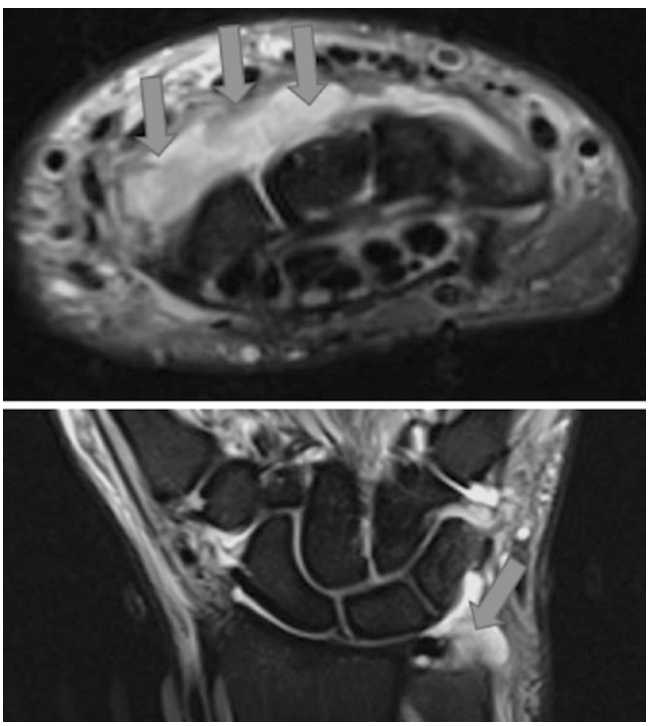

Fig. 4.22 Axial and coronal fluid-sensitive MR images demonstrate joint effusion and evidence of synovitis (arrows) involving the distal radioulnar joints and midcarpal joints compatible with inflammatory arthropathy

- Diagnosis is best made by a combination of imaging modalities, with radiography suited to defining alignment and osseous abnormalities. CT better depicts radiographically occult fractures, MRI best depicts the soft tissue support structures as well as abnormalities of the bone marrow, and ultrasound is suitable for a dynamic assessment of the tendons and ligaments.

References

1. Chang AL, Yu HJ, von Borstel D, Nozaki T, Horiuchi S, Terada Y, et al. Advanced imaging techniques of the wrist. Am J Roentgenol. 2017;209(3):497–510.
2. Taghinia AH, Talbot SG. Phalangeal and metacarpal fractures. Clin Plast Surg. 2019;46(3):415–23.
3. Lamaris GA, Matthew MK. The diagnosis and management of mallet finger injuries. Hand. 2017;12(3):223–8.
4. Elzinga KE, Chung KC. Finger injuries in football and rugby. Hand Clin. 2017;33(1):149–60.
5. Christie BM, Michelotti BF. Fractures of the carpal bones. Clin Plast Surg. 2019;46(3):469–77.
6. Scalcione LR, Gimber LH, Ho AM, Johnston SS, Sheppard JE, Taljanovic MS. Spectrum of carpal dislocations and fracture-dislocations: imaging and management. Am J Roentgenol. 2014;203(3):541–50.

7. Mayfield JK, Johnson RP, Kilcoyne RK. Carpal dislocations: pathomechanics and progressive perilunar instability. J Hand Surg Am. 1980;5(3):226–41.
8. Kani KK, Mulcahy H, Chew FS. Understanding carpal instability: a radiographic perspective. Skelet Radiol. 2016;45(8):1031–43.
9. Wright TW, Dobyns JH, Linscheid RL, Macksoud W, Siegert J. Carpal instability non-dissociative. J Hand Surg Br. 1994;19(6):763–73.
10. Saldana MJ. Trigger digits: diagnosis and treatment. J Am Acad Orthop Surg. 2001;9(4) Available from: https://pubmed.ncbi.nlm.nih.gov/11476534/
11. Adams JE, Habbu R. Tendinopathies of the hand and wrist. J Am Acad Orthop Surg. 2015;23(12):741–50.
12. Lark ME, Maroukis BL, Chung KC. The Stener lesion: historical perspective and evolution of diagnostic criteria. Hand. 2017;12(3):283–9.
13. Garcia-Elias M, Puig de la Bellacasa I, Schouten C. Carpal ligaments: a functional classification. Hand Clin. 2017 Aug;33(3):511–20.
14. Acott TR, Greenberg JA. Ulnar abutment syndrome in the athlete. Orthop Clin North Am. 2020;51(2):227–33.
15. Ko JH, Wiedrich TA. Triangular fibrocartilage complex injuries in the elite athlete. Hand Clin. 2012;28(3):307–21. viii
16. Kirchberger MC, Unglaub F, Mühldorfer-Fodor M, Pillukat T, Hahn P, Müller LP, et al. Update TFCC: histology and pathology, classification, examination and diagnostics. Arch Orthop Trauma Surg. 2015;135(3):427–37.
17. Tomaino MM, Elfar J. Ulnar impaction syndrome. Hand Clin. 2005;21(4):567–75.
18. Bell MJ, Hill RJ, McMurtry RY. Ulnar impingement syndrome. J Bone Joint Surg Br. 1985;67(1):126–9.
19. Cerezal L, del Piñal F, Abascal F, García-Valtuille R, Pereda T, Canga A. Imaging findings in ulnar-sided wrist impaction syndromes. Radiographics. 2002;22(1):105–21.